Estuaries and Coasts (2024) 47:1359–1375
https://doi.org/10.1007/s12237-024-01376-1

MANAGEMENT APPLICATIONS

Evaluating Coastal Wetland Restoration Using Drones and High-Resolution Imagery

J. Mason Harris[1] · Whitney P. Broussard III[2] · James A. Nelson[3]

Received: 24 January 2024 / Revised: 2 May 2024 / Accepted: 13 May 2024 / Published online: 24 June 2024

Abstract

Coastal marsh ecosystems are changing and being lost at a rapid rate around the world. One of the fastest rates of land loss, specifically coastal marsh habitat, occurs in Louisiana on the Northern Gulf Coast of the USA. To address this issue, state and federal agencies have undertaken massive wetland restoration efforts to preserve and restore coastal marsh habitats in Louisiana. For these efforts to be successful in the long-term, it is critical to understand what methodologies and techniques result in resilient restoration projects. However, traditional methods to monitor restoration success rely on labor intensive field measurements that are often limited in scope, difficult to maintain, and underfunded. Recent technological developments with uncrewed aircraft systems (UASs) and image processing have substantially improved the ability of restoration practitioners to use off-the-shelf UASs and cameras to map projects. We present a streamlined method using a commercially available drone with a high-resolution red, green, blue (RGB) camera to assess the effects of wetland restoration and integrate more modern tools into evaluation approaches. We conducted drone flights at restored brackish marshes of various ages using a space for time substitution with the goal of understanding the long-term success of marsh restoration. We observed that created marshes had higher land to water ratios than natural marshes. This finding suggests that these restored areas were gaining and maintaining elevation after approximately 10 years. Our method shows that drone surveys offer low-cost, minimally invasive methods for evaluating restored wetlands and ultimately tell us more about ecosystem function through realistic site-level habitat configurations.

Keywords Spartina · Louisiana · Saltmarsh · UAS · Drone · Object-Based Image Analysis · Habitat Mapping

Introduction

Wetlands are some of the most indispensable ecosystems on the planet. The unique environments are widely recognized for supporting fish and wildlife production and maintaining biodiversity. Wetlands are also the filters and regulators of water on the landscape because they are the downstream receivers that absorb pollution, temporarily store floodwaters, and recharge groundwater aquifers (Mitsch and Gosselink 2015). Carbon sequestration in wetlands is also an essential function to mitigate effects of greenhouse gases and global climate change. Although wetlands cover only 5–8% of terrestrial environments, they contain 20–30% of the earth's soil pool of carbon (Mitsch et al. 2013). Wetlands benefit many organisms but also many other habitats.

Coastal estuaries and marshes provide economic and cultural benefits like buffering storm impacts, supporting commercial fisheries, and promoting recreation and tourism (Barbier et al. 2011). In 2010, 39% of Americans (123.3 million people) lived in coastal counties which comprise less than 10% of the total land area in the USA (Crossett et al. 2013). And this was expected to increase 8% (10 million people) by 2030. Coastal communities and economies need healthy intact wetlands to protect valuable fisheries, port facilities, tourist destinations, and energy infrastructure.

Communicated by Richard C. Zimmerman

✉ James A. Nelson
jimmy.nelson@uga.edu

J. Mason Harris
jmason.harris@duke.edu

Whitney P. Broussard III
whitney.broussard@freese.com

[1] Department of Biology, University of Louisiana at Lafayette, 410 E. St. Mary Blvd., Lafayette, LA 70504, USA

[2] Freese and Nichols, Inc, 314 Jefferson St., Lafayette, LA 70501, USA

[3] Department of Marine Sciences, University of Georgia, 325 Sanford Dr., Athens, GA 30602, USA

Coastal wetlands in the USA were calculated to contribute $23.2 billion per year in storm protection, and a loss of 1 ha of wetland can lead to a $33,000 increase in damage from some storms (Costanza et al. 2008). Despite some marshes showing signs of resiliency, many coastal wetlands are facing major global threats as a result of human activity and climate related impacts (Millennium Ecosystem Assessment 2005).

Louisiana's coast is an important natural resource that supports cultures, economies, and ecosystems. Marshes make up much of the coastal habitat but are disappearing rapidly. Louisiana's coastal zone has lost approximately 4830 km^2 of wetlands from the 1930s to 2016 (Couvillion et al. 2017). Since roughly 40% of coastal wetlands in the USA are found in Louisiana, this loss accounts for 80% of the national reduction in wetlands in the last century (Boesch et al. 1994). Between 2004 and 2008, more than 775 km^2 of marsh were lost from major hurricanes (Couvillion et al. 2011). The accelerated loss in Louisiana, however, is caused by a combination of factors including Mississippi river levees, oil and gas exploration, channel construction, subsidence, and sea level rise.

Due to the rapid loss of these valuable areas, the state of Louisiana is planning $50 billion worth of restoration projects over the next 50 years to create new habitats and rehabilitate degraded ones (CPRA 2023). A variety of techniques have been employed, such as marsh creation, barrier island restoration, shoreline protection, terracing, diversions, and hydrologic restoration. Coastal Master Plan currently includes the nation's largest investment in marsh creation at $16 billion over the next 50 years. Since this technique typically consists of creating a new wetland out of a shallow water area, rather than rehabilitating a degraded one, understanding how these areas function as wetland habitats is critical to implementing better restoration techniques in the future.

Off-the-shelf uncrewed aircraft systems (UASs), commonly referred to as drones, are being increasingly used in environmental assessments. The technology offers monitoring solutions for areas that are difficult to access and greatly benefit from high-resolution maps, like restored coastal wetlands. Traditional methods for monitoring restored wetlands are time and labor intensive and often fail to provide holistic site assessments. Data captured by regular RGB cameras standard with most modern drones can significantly improve our understanding of restoration progress and the development of a site over time. Multispectral, Light Detection and Ranging (LiDAR) and other precision sensors or cameras are highly beneficial for landscape and vegetation analysis but are not widely available to everyone (Colomina and Molina 2014). Although many studies have used drones and remote sensing to assess wetlands, few have used them specifically for understanding wetland restoration (Boon et al. 2016; Broussard et al. 2018; Broussard et al. 2022; Doughty and Cavanaugh 2019; Husson et al. 2016; Kalacksa et al. 2017; Pande-Chhetri et al. 2017; Zweig et al. 2015). Drones fill a niche in remote sensing with higher resolutions and greater operational flexibility than manned aircrafts or satellites at a much lower cost, albeit with greatly reduced areal coverage (Klemas 2015). Processing techniques like photogrammetry can create multiple data types from drone images, like 3-layer RGB mosaics and digital surface models, that can be used to make accurate site maps and vegetation classifications (Husson et al. 2017). The technology is a powerful tool for restoration managers and ultimately provides better knowledge of site development than most traditional surveys.

Field surveys are an essential part of restoration monitoring. They are also necessary to ground truth remote sensing data. Field measurements for restoration monitoring in Louisiana typically include things like species composition, percent cover, and vegetation height (Folse et al. 2014). Plant identities inform managers on patterns of succession and rates of community change that in theory should ultimately reach some stable climax ecosystem with desired types of plants. And restoration projects aim to mimic a natural reference area or a pre-existing state using species compositions as a critical metric to determine success. Visual cover estimates, however, are subjective and are often conducted at random stations or along transects that can fail to fully capture a site. This ground data, however, can also be used for training software to detect these species at much broader scales (Broussard et al. 2022).

By combining field surveys and UAS imagery, researchers can use holistic site assessments to understand ecological progression and restored function in wetlands. Doughty and Cavanaugh (2019) integrated the two approaches to estimate aboveground biomass in saltmarshes and monitor seasonal changes in productivity. In a restoration context, vegetation classifications and site assessments using principles of landscape ecology will inform development over time. Accurate mapping and spatial analysis of water bodies will help researchers understand site evolution since tidal drainage and channels are important marsh landscape components (Weinstein et al. 2001). Hydrology is also considered the master variable in structuring plant communities and contributing to overall restoration success, and spatial resolution has an impact on mapping of smaller water bodies (Mitsch and Gosselink 2015; Enwright et al. 2014).

Here, we combined drone flights and field surveys to assess restoration sites along a chronological sequence of marsh creation in the Lake Sabine National Wildlife Refuge in southwest LA, USA. We chose four neighboring restoration projects completed from 2002 to 2015 using a space for time substitution to understand changes in the restoration sites overtime. We also mapped and sampled two natural

marshes adjacent to the marsh creation sites for reference comparisons. The aim of the study was to (1) determine how similar restored and reference locations were in physical and biological characteristics over time, (2) evaluate whether drone-based structural assessments and landscape metrics correlate with species distributions and site age, and (3) assess the restored and reference comparisons to infer if the restored sites became more similar to the reference sites over time as a measure of restoration success.

A secondary goal was to develop methods to improve wetland restoration assessments using off-the-shelf drone technology. We assess species compositions, land/water ratios, and other landscape metrics (e.g., edge and fragmentation indices), which are widely used in remote sensing studies to determine their efficacy for determining the ecological success of restoration (Couvillion et al. 2016). Our hope is that this work provides managers and practitioners easily accessible methods to document and assess restoration successes and failures.

Methods

Study Sites

This study occurred in Sabine National Wildlife Refuge, Cameron Parish, LA, USA, on the site of the Louisiana Coastal Wetlands Planning, Protection, Restoration Act's (CWPPRA) Sabine Refuge Marsh Creation Project (CS-28 Cycles 1–5). The restoration was originally approved by the US Army Corps of Engineers in 1999, and later, the project was broken into five "cycles" of marsh creation. The area is a mixture of natural and restored brackish marsh and shallow open water that experienced significant land loss due to canal building, altered hydrology, saltwater intrusion, and hurricanes (Louisiana Coastal Wetlands Conservation and Restoration Task Force 2012) (Fig. 1). The Louisiana Coastal Protection and Restoration Authority (CPRA), US Army Corps of Engineers, and US Fish and Wildlife Service partnered to carry out restoration efforts for each cycle. Construction practices for each cycle were generally consistent, but with some variation. The boundary of each site was determined in the project planning phase. The initial phase of construction involved building earthen levees to create the containment areas for each cycle. In general, dredge spoil slurry from the shipping channel was pumped into containment dikes to a maximum height of 70 cm (NAVD88 Geoid 12 A) and expected to settle to a height of 9 cm after 5 years. Note our analysis uses the current Geoid 18 which addresses the issue of subsidence-related error in elevation estimates from Geoid 12 A. Each site had a sediment "overflow" component where the containment dike was breached along the lakeside levee to allow extra dredge material to flow out into open water and create additional marsh, but the technique only worked once. Typically, tall stands of smooth cordgrass (*Spartina alterniflora*) expanded in the first few years, taking each site about 3–4 years to become > 70% vegetated.

The cycles were completed between 2002 and 2015. The timeline is as follows: Cycle 1 was finished in 2002, Cycle 3 in 2007 (note Cycle 3 was completed before Cycle 2), Cycle 2 in 2010, and Cycle 5 in 2015. Unfortunately, one site (Cycle 4) was excluded from this study due to complications with the imagery.

Cycle 1 had an original containment of 87 ha and was completed in February 2002. It is the oldest restoration site in this study (17 years). The site was pumped to an elevation of 55–67 cm (Sharp 2011); settled elevation was 14 cm after 7 years (April 2009) and has been accreting at a rate of 0.4 cm/year since 2010. The most recent average elevation reading was 22 cm (CRMS 2019). Cycle 1 was the only site to be planted and have trenasses (small man-made channels) manually dug during construction. Thirty-six thousand *S. alterniflora* sprouts were planted along the perimeter and trenasses. The site was 86% vegetated land after about 8 years and 94% land after 14 years, surpassing its goal of creating 50 ha of marsh (Miller 2014; Beck et al. 2019). *S. alterniflora* was the dominant species until after about 7 years when the community diversified to include seashore saltgrass (*Distichlis spicata*), saltmarsh bulrush (*Schoenoplectus robustus*), bulrush (*Schoenoplectus americanus*), and saltmeadow cordgrass (*Spartina patens*). Monitoring was conducted by CPRA until a coastwide reference monitoring station (CRMS 6301) was established in 2009.

Cycle 3 was initially 93 ha and completed in May of 2007. It was pumped to an initial elevation of 12–61 cm. Pumping errors caused the site to be higher in the south and lower in the north with a wide range of surface elevations. Levees were breached every 150 m on the northwest side for the overflow technique, but it failed. Settled elevations were surveyed between −62 and 24 cm after 6 years with the majority of transects below targets; however, most transects were above the 9 cm goal after 11 years. The project area was 4.5% vegetated land after 2 years and 97.8% land after 8 years (Miller et al. 2019; Beck et al. 2019). *S. alterniflora* was the dominant plant during early colonization, like Cycle 1, and Virginia glasswort (*Salicornia depresa*) established some stands initially but disappeared after a few years. Vegetation diversified 8 years after construction with the emergence of *D. spicata*, *S. robustus*, and others, but *S. alterniflora* remained dominant through 2018.

Cycle 2 had a containment area of 93 ha and was completed in May 2010. There is limited construction and historical monitoring data because it was converted to a state-only project with no monitoring budget. The only available data is aerial imagery from 2015 and Suir et al. (2020) satellite imagery. Unlike other sites, the "overflow" component was

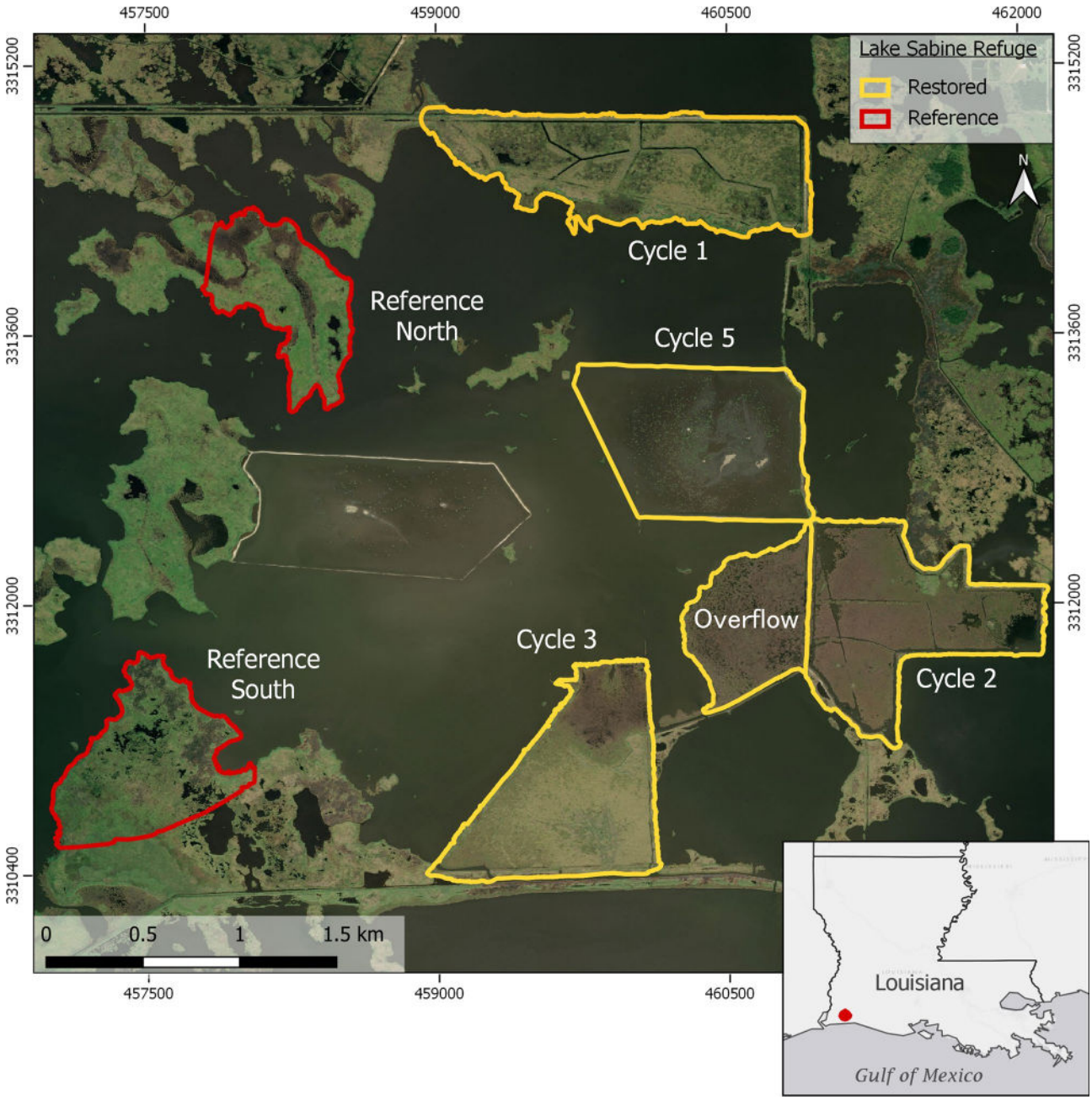

Fig. 1 Location of study sites (Cycles) in the Lake Sabine National Wildlife Refuge

successful and created more than 40 additional hectares of marsh outside the levees. This area will be referred to as Cycle 2 overflow. It is reported the elevations were pumped too high initially, based on personal communication with restoration managers and researchers, and that extra sediment probably contributed to the overflow success. The site has been a *S. alterniflora* monoculture, and it was 77% land in 2015 (Suir et al. 2020; Beck et al. 2019).

Cycle 5 was 94 ha and was finished in March 2015 with no initial elevation reported (Pontiff and White 2017). Three years after construction in 2018, the elevation settled to between −12 and 26 cm (Miller et al. 2019). Vegetation expanded rapidly post-construction, and the site was 64% vegetated land within 9 months. *S. alterniflora* was the dominant species with nominal percentages of other plants. Monitoring reports also point out that the containment dike

along the western edge has several major gaps, more than other sites, possibly resulting from erosion or initial construction practices.

We used two nearby natural marshes as reference areas for our comparisons. We chose them because they have been previously monitored by restoration agencies and are the largest stretches of marsh in the area. Reference North is a 50-ha marsh dominated by *Spartina patens* with swathes of *Spartina alterniflora* along its larger tidal sections and smaller amounts of *Schoenoplectus robustus*, *Schoenoplectus americanus*, and *Eleocharis* spp. across the site. Reference South is a 66-ha *Spartina patens*–dominated marsh with pockets of water scattered across the interior of the site.

Planning and Field Work

All flights were conducted using a multi-rotor platform (Yuneec H520). This hexacopter aircraft was designed for commercial use and chosen for the study because of high wind resistance, stability, and flight time (28 min). The H520 was equipped with an integrated autopilot system accessed through Yuneec's mission planning software (DataPilot). The hover accuracy of the aircraft using uncorrected Global Positioning System (GPS) measurements was 1.5 m horizontal and 0.5 m vertical. The internal GPS module geotagged images with an initial orientation accuracy of 5 m horizontal and 8 m vertical. Flight times ranged from 15 to 23 min.

A Yuneec E90 RGB camera was used to record images. Its 23-mm lens provided wide angle views with low distortion and increased sensitivity in low-light conditions. The diagonal field of view was 91°. The camera had a 1″ CMOS sensor, and its rolling shutter operated at 1/8000–4 s. Photo resolution was 3:2 (5472 × 3648), and effective resolution was 20 MP. Photo format was 10–12 MB JPEG files, and the coordinate reference system was WGS84 UTM Zone 15 N.

The flight plans were developed using Yuneec DataPilot desktop mission planning software. All flights were conducted at 68 m altitude above ground level using consecutive transects to cover the survey areas with an image overlap of 80% (frontlap and sidelap) and speed of 5 m/s. This altitude was chosen to maximize field of view while achieving < 2.5 cm GSD (ground sample distance) or pixel resolution in the final maps for a precise analysis of vegetation classes and to minimize possible blurred portions (Broussard et al. 2022).

We installed ground control points (GCPs) at each site with one near approximate site center in addition to random checkpoints. GCPs are used to georeferenced the model, and checkpoints are used to assess the final absolute accuracy. Typically, 6 GCPs and 3 checkpoints were used at each site based on photogrammetry software manufacturer recommendations (Pix4D Mapper) and previous studies (Manfreda et al. 2019; Oniga et al. 2018). Coordinates were measured with a Trimble R10 GNSS unit, utilizing real-time kinematic corrections (RTK), to ensure precise geolocation of GCPs and final products. Horizontal error ranged from 1 to 15 cm and vertical error between 1 and 25 cm. The x, y, and z coordinates of 69 points were taken with an overall mean error of 1.2 cm horizontal and 2.1 cm vertical. In total, 46 targets were used as control points for georeferencing the imagery, and 23 targets were reserved as horizontal and vertical checkpoints to help assess accuracy of the data. Point data was compiled into .CSV files at each site for processing within the Pix4D photogrammetry software. We conducted drone flights in the summer of 2019 from late June–mid-July between approximately 9:30 am and 1:30 pm CST. In total, 37 flights were conducted.

Ground Truth Surveys

We conducted surveys to verify the remotely sensed data and compare the sites using traditional monitoring methods (Fig. 2). Nine 2 × 2 m quadrats were surveyed at each site for species composition, plant height, and percent cover of vegetated and unvegetated surface. We used a Braun-Blanquet cover scale used by the USGS Coastwide Reference Monitoring System (CRMS) and CPRA that have been used to monitor these sites in the past (Folse et al. 2014; Miller 2014).

Processing and Analysis

The flight images were mosaicked within the software Pix4D Mapper (version 4.4.12) to create orthomosaics and 2.5D digital surface models (DSMs) using Structure from Motion (SfM) algorithms. The SfM technique has revolutionized analyzing surface structure in ecology and is perhaps the most practical and affordable alternative to LiDAR (Forsmoo et al. 2019). We only used the DSMs in this study to aid in vegetation classification using the parameter for plant height only.

Once images were uploaded, the software detected camera parameters, image coordinate system, altitude, and location details for each picture. The coordinate system output for the orthomosaics was WGS84 UTM zone 15 N. We used the 3D maps processing template in Pix4D to create an orthomosaic, point cloud, and DSM. GCP and checkpoint measurements were uploaded with x, y, and z coordinates and horizontal and vertical precision error values, and the targets were verified using the ray cloud editor. Manual tie points (MTPs) were also added in the ray cloud to improve reconstruction accuracy and clarity in the final orthomosaic. MTPs are points created after initial processing by marking or clicking the exact same point at a site in multiple images. Processing was conducted on a Dell Precision Tower 5810 desktop with 32

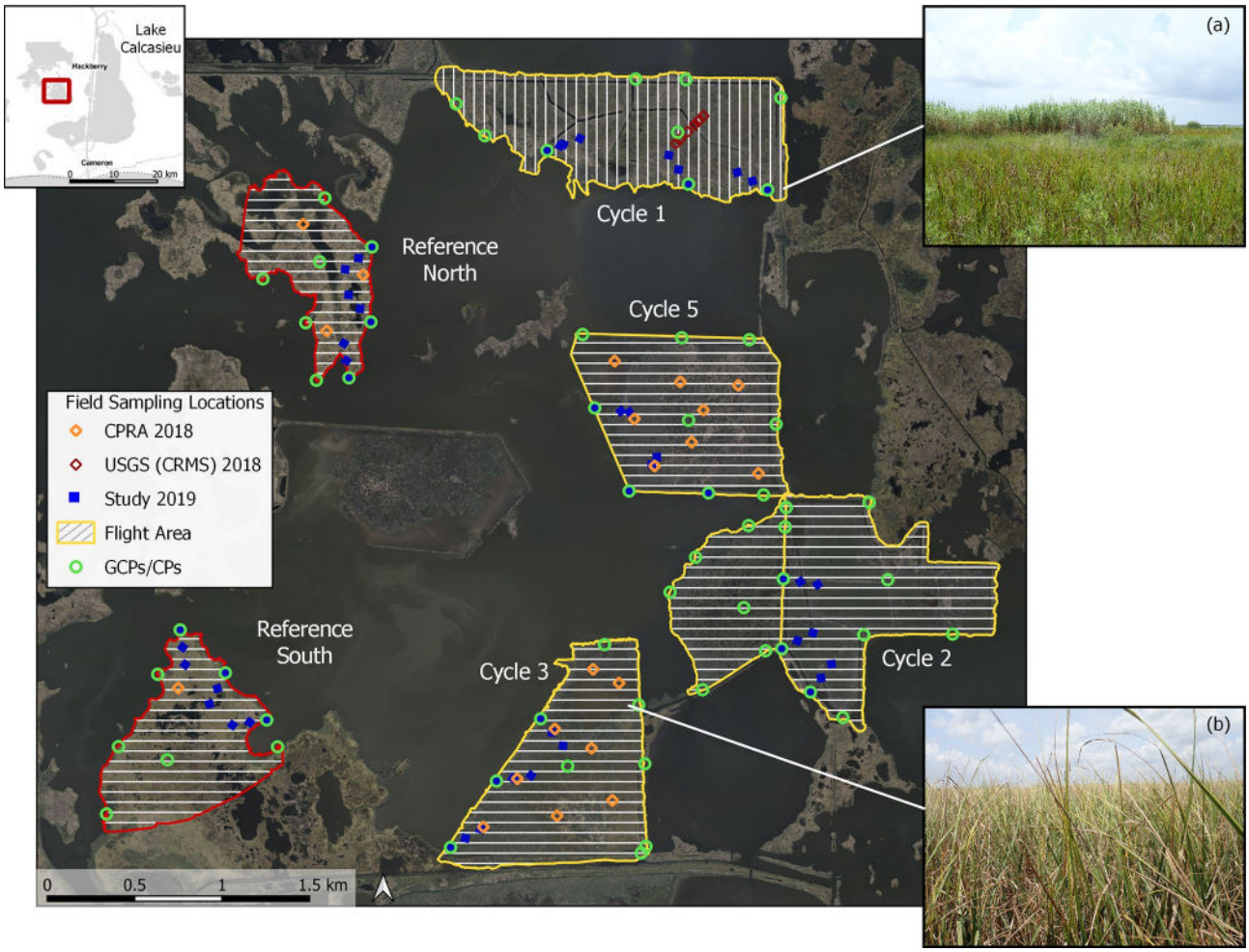

Fig. 2 Field sampling locations and flight areas covered by the Yuneec H520. Examples of vegetation include: a mixture of *Spartina alterniflora*, *Schoenoplectus robustus*, and *Distichlis spicata* in the foreground with taller *Phragmites australis* in the background (**a**) and *Spartina alterniflora* (**b**)

GB of RAM (random-access memory), an Intel Xeon CPU E5-1603 v3 @ 2.80 GHz, and a NVIDIA Quadro M2000 GPU. Processing times ranged from 18 to 72 h per site. A total of 20,515 raw images were processed to create 686 ha of mapped area with an average pixel size of ~ 2.2 cm (excluding Cycle 4).

Two products were created by combining the orthomosaics and DSMs: (1) land/water maps and (2) vegetation species/dominant group classifications. Classes were assigned based on the ground reference data. Land and water classes were delineated based on rules developed by Cowardin et al. (1979) where land was considered all vegetation including marsh, scrub/shrub, emergent vegetation, and exposed bare ground on the containment dikes (which is higher elevation and does not flood). Water was considered open water, nonvegetated mud flats, floating aquatics, and submerged aquatic vegetation.

The vegetation on each site was classified into one of the following six classes identified from the ground surveys: bare ground, *D. spicata*/*S. patens*, *Phragmites australis*, *Spartina alterniflora*, scrub shrub, and water. Bare ground was considered exposed, unvegetated bare soil on containment dikes. The *D. spicata*/*S. patens* class represented vegetation stands where *Distichlis spicata* or *Spartina patens* were the dominant species. These two vegetation types were difficult to distinguish at the restored sites so fithe species were grouped, although *D. spicata* was more common based on field surveys. Often, these stands were mixed with smaller percentages of *Schoenoplectus robustus* or *Schoenoplectus americanus* with nominal percentages of other species. The *Phragmites australis* class represents roseau cane or common reed which is a grass that forms dense stands reaching heights of 1–6 m. *Spartina alterniflora* represents vegetation stands where smooth cordgrass was the dominant species. *S. alterniflora* was sometimes mixed with *S. robustus* and other species. Scrub shrub primarily consisted of Jesuit's bark (*Iva frutescens*). The reference sites contained

similar classes, but both had a *Spartina patens* category because it is the dominant species at both sites. Reference North also had an *Eleocharis* spp. class because it contained a few dense stands of the vegetation.

To classify the orthomosaic images by vegetation type, an object-based image analysis (OBIA) approach was used to conduct vegetation mapping with the software eCognition Developer (v. 9.5, Trimble Germany GmbH, Munich, Germany). Orthomosaics and digital surface models (DSM) provided four layers to use in the image analysis based on natural color reflectance values and the surface model (red, green, blue, & DSM). Individual "rulesets" were developed for each site using similar approaches and parameters to assign classes to cover types. Rulesets are a step-by-step process of segmentation (grouping pixels into meaningful shapes, e.g., water bodies or trees) to create objects, and classification of those objects based on attributes or "features." Cycles 3 and 5 and Reference South were completely automated using ruleset development which included a supervised classification as the last step to separate grass species (after other classes had been identified using threshold values of various features), and no manual editing was performed. The other three sites were initially classified into grass, *Phragmites*, bare ground, and water using basic rules and manual editing. From these initial classifications, water, *Phragmites*, and bare ground were preserved, and the grass class was segmented and classified following methods for the other sites. Although the techniques varied slightly, comparisons across sites were valid because spatial resolutions are identical (~ 2.2 cm GSD) and overall accuracies were similar.

The three automated sites (Cycle 3, Cycle 5, and Reference South) were analyzed by running segmentation algorithms for each class of interest. Segmentation is a key step because its outcomes have a significant impact on accuracy (Dronova 2015). It was a subjective process of trial and error to find the right combination of scale, color/shape, and compactness/smoothness within the "Multiresolution Segmentation" algorithm which is a common problem in OBIA (Baatz and Shaape 2000). All sites began with the classification of water. A multiresolution algorithm using scale parameter of 30, shape 0.3, and compactness 0.75 (with only red, green, and blue layers) followed by a spectral difference segmentation using a scale of 5 (using all layers, including DSM) yielded the best results for separating water from vegetated marsh. The addition of the spectral difference algorithm helped increase the object size for larger water bodies, making classification easier with fewer objects, while still capturing small pockets and channels that were important for fine-scale analysis. The texture feature Gray Level Co-occurrence Matrix Homogeneity (all directions) and the spectral features normalized difference index (NDI) green–blue and mean brightness were the most useful for initially classifying water (Husson et al. 2016; Laliberte and Rango 2011). NDI green–blue is the NDI of the mean values of the 2 bands adapted from Hunt et al. (2005).

$$\mathrm{NDI} = \frac{\mathrm{Green} - \mathrm{Blue}}{\mathrm{Green} + \mathrm{Blue}}$$

NDI values for other band combinations were used to identify vegetation later in the process. Bare ground was sometimes misclassified as water but could typically be separated using high mean brightness values, sometimes texture, and distance to scene border because the only bare ground was along the containment dikes. Remaining unclassified objects were merged and segmented for the next class. *Phragmites* was next because it could typically be identified using the mean DSM values. *Phragmites* was generally much taller than surrounding plants in these marshes. Objects with a mean DSM value of greater than or equal to 1–2 m were usually assigned to the *Phragmites* class. A multiresolution algorithm with a scale parameter of between 100 and 150, shape 0.3, and compactness 0.75 produced the best results for segmenting *Phragmites*. An issue with the use of DSM values was that several of the sites had flaws in the surface models. This was overcome by using x and y distance to scene borders for target areas. It is possible that smoothing or resampling the surface models to a lower resolution would help overcome this issue, but our method was quick and effective for reducing misclassifications. Rules used to refine initial classifications for *Phragmites* included relative border to *Phragmites*, a mean DSM value of around 1.5 m, and mean brightness. Scrub shrub was next, and in some cases, the same segmentation for *Phragmites* was used. Otherwise, objects were merged and segmented with another multiresolution algorithm using scale parameter of 50, shape 0.3, and compactness 0.75. Objects with a mean DSM greater than 1 m were initially classified as scrub shrub and refining rules utilized the mean difference to neighbors DSM and textural features. Lastly, a spectral difference algorithm with a maximum spectral difference of 3–10 was applied to segment and enlarge remaining unclassified objects. The last 2 classes analyzed were *Spartina alterniflora* and *D. spicata*/*S. patens* (*Spartina patens* and other for Reference South). Training samples of each were selected, and a nearest neighbor supervised classification was performed based on similarities of four features: NDI green–red, brightness, mean DSM, and area.

The first three sites that were analyzed (Cycle 1, Cycle 2, and Reference North) were done using one round of segmentation; basic rules to separate bare ground, marsh vegetation, water, and *Phragmites*; and additional manual editing. The parameters for the multiresolution segmentation were scale 150, shape 0.3, and compactness 0.75. Initial features used to define classes were mean brightness, mean red band, mean DSM, roundness, area, and position values for individual

objects. Misclassified areas were identified and reclassified through additional thresholding of other parameters or manually edited into the appropriate cover type. Water, bare ground, and *Phragmites* classes were retained for these sites, and the remaining vegetation was classified using the same methods for the automated sites.

We exported classifications as polygon layers with area (m^2) and border length (m) included as attributes. Accuracy assessments consisted of approximately 500 stratified random sampling points per site using ArcMap (10.4.1). We created an error matrix for each site using orthomosaics as reference datasets for determining classification accuracy (Congalton 1991). All border length and area statistics were aggregated and analyzed in R using the Tidyverse package (v 3.5.1, R Development Core Team).

Remotely sensed class areas, percentage of landscape, number of patches, patch density, edge density, and aggregation index (AI) were calculated based on usage in previous studies (Broussard et al. 2018). Land and water classes were resized to 5-cm resolution for calculations. A patch was defined as a habitat unit that differed from its surroundings based on the resolution of the files (e.g., a piece of land isolated by water). AI has become a widely used metric for evaluating landscape structure and is a percentage calculated from the ratio of the observed number of patch type adjacencies (McGarigal 2015; Couvillion et al. 2016). The number of patches is an indicator of the fragmentation of a class based on the total number of isolated patches present on the landscape. Patch density is the number of patches per unit area based on total landscape area in square meters. Edge density is the amount of edge per unit area, standardized for comparisons across areas of different sizes. Edge habitat in this study was considered to be the marsh-to-water border. Since the sites were cropped to the marsh edge and no water was classified outside the boundaries, the border length of the water class was used as a proxy for interior edge habitat. Exterior edge habitat was then the total length of the land class minus the amount of interior. Portions where continuous habitat was cut off due to flight coverage were measured and subtracted from total edge calculations. All landscape configuration metrics were calculated in R using the Landscapemetrics package.

Floristic Quality Index (FQI) provides an estimate of wetland quality based on species composition and percent cover of a plant community (Gianopulos 2014). FQI is scored from 0 to 100 (following CRMS protocol) using coefficient of conservatism (CC) values assigned to specific plants by a panel of coastal vegetation experts. CC values are regionally or state specific and plants are also assigned to general classes: invasive species (CC = 0), disturbance species (CC = 1–3), less vigorous communities (CC = 4–6), common vigorous communities (CC = 7–8), and dominant species (CC = 9–10) (Suir and Sasser 2017). Scores used in this study were based on the ones used by Suir et al. (2020). Modified Floristic Quality Index (FQI_{mod}) was calculated using field survey data to compare to CRMS and CWPPRA metrics using the formula:

$$FQI_{modt} = \left(\frac{\sum \left(COVER_{it} \times CC_i \right)}{100} \right) \times 10,$$

where $COVER_{it}$ is the percent cover for particular species i at a sample unit in a sample site at time t, and CC_i is the coefficient of conservatism value for species i (Cretini et al. 2011). The index has been shown to be useful for assessing wetland restoration maturation and detect plant community changes over time (Lopez and Fennessy 2002).

We compared these results with previous analysis of the sites conducted by monitoring agencies and Suir et al. (2020). Field monitoring data was compared to information from CPRA surveys in 2018, CRMS data from 2018, and data from 2015 that consisted of species composition, percent cover, and FQI calculations. CRMS is a statewide network of stations to provide data for restoration decision-making. UAS data was compared to land water classifications of 1-m resolution aerial imagery (USGS) acquired in late 2015 and 0.31–1.2 m resolution WorldView-3 imagery acquired in early 2016. UAS classifications of the restoration sites were masked to same extent as the satellite data using shapefiles from the previous study.

Results

The land/water classifications calculated the restoration sites were between 73 and 96% land (Figs. 3 and 4, Table 1). The youngest restoration site (Cycle 5) was the lowest at 73.2% land, and the oldest site (Cycle 1) had the highest coverage at 95.5% land. The two middle-aged sites (Cycles 2 & 3) were even at 86.5% and 86.4% land, respectively. The land/water analysis revealed that the marsh creation sites exhibited rapid expansion of vegetated land in the first 4 years post-construction (18 %/year) and then gradually for the next 10–12 years (2.4 %/year) until sites surpassed proportions of reference marshes (Fig. 3). These findings support previous remote sensing analysis of the restoration sites in regard to percentages and rates of expansion over time (Beck et al. 2019; Miller 2014; Suir et al. 2020). Cycle 2 created the most marsh due to the success of the overflow technique (48 ha). The reference sites (North & South) were also close in configuration at 91% and 92% land, respectively (Figs. 3 and 4).

The younger restoration sites were dominated by *Spartina alterniflora* while the older sites showed a pattern of more mixed vegetation types with higher amounts of *D. spicata*/*S. patens* (Fig. 5). In general, the restored sites exhibited rapid

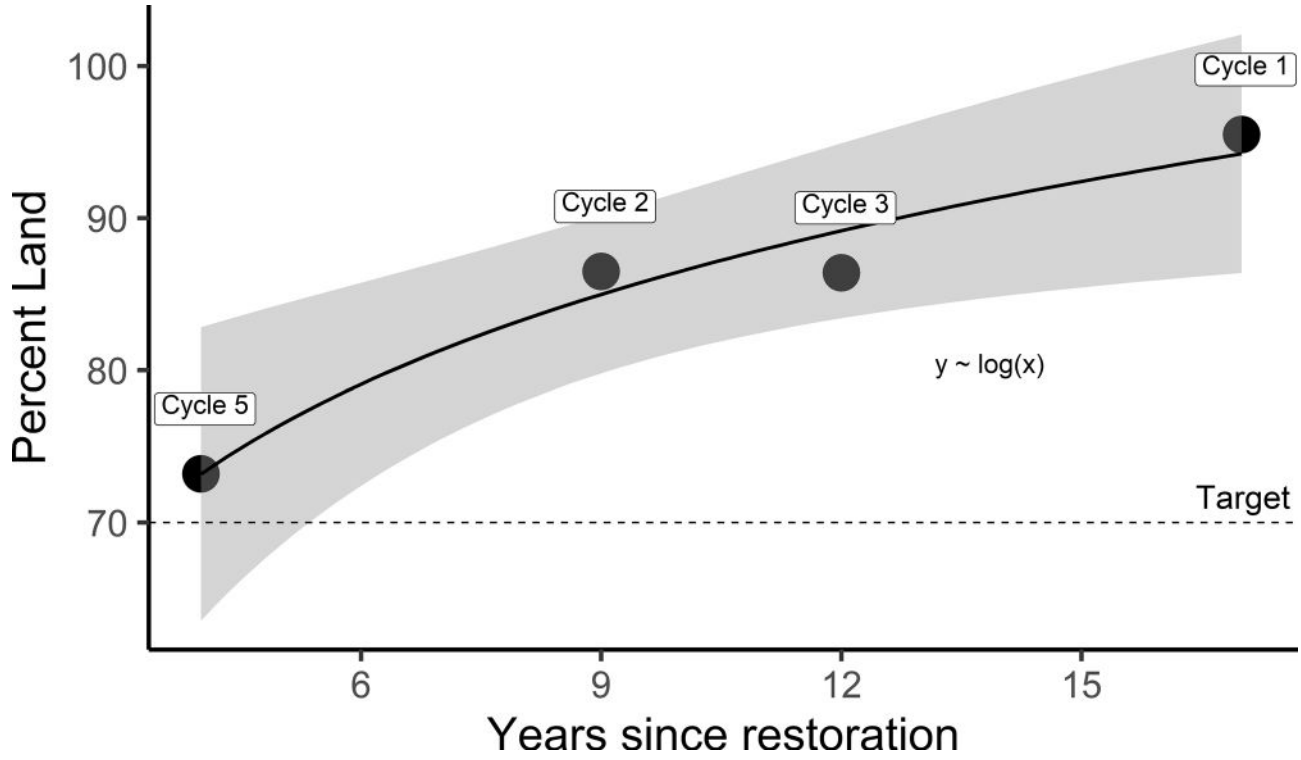

Fig. 3 Drone-based percent land cover for restored sites over time since restoration

invasion of *Spartina alterniflora* in the first 10 years followed by an expansion of *Distichlis spicata*, *Spartina patens*, and *Schoenoplectus robustus* with small percentages of other species. The two younger sites, Cycles 5 and 2, were 64% and 76% *Spartina alterniflora* (Fig. 6). The two older sites, Cycles 1 and 3, were 36% and 31% *Spartina alterniflora*. In contrast, the reference sites were dominated by *Spartina patens*; North was 67% and South was 78% *S. patens*. Reference North had 14% *Spartina alterniflora* cover, and Reference South did not have any. Overall accuracies for the classifications were between 75 and 90% with a mean overall accuracy of 83%. Kappa values ranged 0.54–0.82 with an overall mean of 0.68. We achieved the highest accuracy, 90% overall, at the two youngest restoration sites probably because they had less diverse vegetation communities. The least accurate classification was 75% at Cycle 1 which had the highest average species richness . Representative photos along with their corresponding classifications are in Fig. 7 for visual comparison.

The field survey-based species assemblage of the restoration sites reflected the drone-based dominant species classifications (Fig. 8). Cycle 3 had a higher amount of *S. patens* than any other restoration area, but this could be due to sampling location bias as a result of site accessibility. Previous studies found a higher percentage of *D. spicata* (Miller 2014). We observed a general trend of increasing diversity and percent vegetated cover over time with Cycle 1 containing a higher number of species on average than the reference locations. Cycle 2 created by far the most marsh but had the lowest species richness with one species per site on average. The older restoration sites, Cycles 1 and 3, had Floristic Quality Index (FQI) scores close to that of Reference South, all between 71 and 74 (Fig. 8). The CRMS monitoring site for Cycle 1 calculated a score of 78 for 2019. Reference North had the highest FQI score of 85, and Cycle 2 had the lowest at 56. FQI is an index of wetland habitat quality based on scores assigned to plants thus ranking their value to the region. The reference sites had an average score of 79 which is close to the ideal score of 80 for Chenier Plain brackish marsh (Cretini et al. 2012). The results of the restored sites indicate the marshes approach this ideal range after about 12 years.

Comparisons to previous remote sensing data show the land water interface calculations were the closest across sensors and years for the most mature restoration site, Cycle 1 (94–96% land) (Table 2). Prior to drone flights in 2019, the most recent remote sensing surveys of the area used 1-m resolution aerial imagery and 0.31–1.24 m satellite imagery from late 2015 and early 2016, respectively. The largest differences occurred with the youngest site, Cycle 5. There was a 35% difference in the amount of land between satellite (29%) and aerial photo (64%) calculations, but this

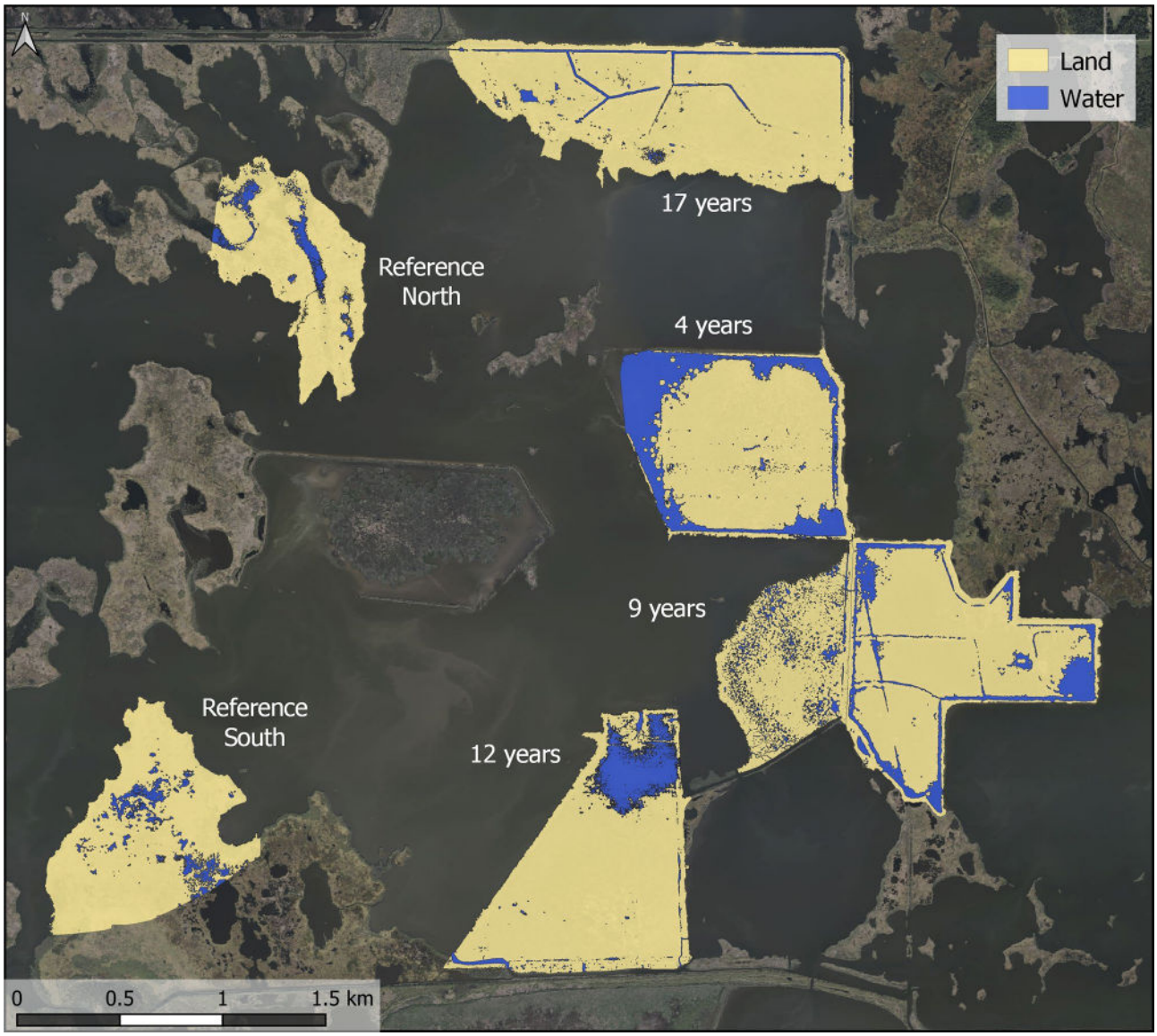

Fig. 4 Drone-based land water interface maps (years since construction as of 2019)

was likely caused by classification methods. Cycle 5 was 73% land by 2019 based on drone data (Table 2). The 2019 drone assessments displayed higher percent land values than previous assessments for all sites except Cycle 3. Estimates decreased from 94 to 98% land in 2015/16 to 86% land in 2019; this was the only site that lost land over time (Table 2).

The dominant species group was the same across sampling techniques at all sites except Cycle 3. Agency field surveys from 2018 (both CRMS and CPRA) estimated *Spartina alterniflora* was the dominant cover type but 2019 drone classifications and personal field surveys estimated *Distichlis spicata/Spartina patens* was the dominant group. Overall, previous vegetation data collected by restoration monitoring agencies and field survey data collected at the same time as the drone flights support the assertion that as sites mature, *Spartina alterniflora* cover declines in these brackish marshes while *Distichlis spicata/Spartina patens* and other vegetation types expand (Miller 2014; Suir et al. 2020).

Table 1 Land/water interface results

Site	Land (ha)	Water (ha)	Total (ha)	% land	% water
Cycle 5	67.6	24.7	92.3	73.2	26.8
Cycle 2	119.3	18.7	138.0	86.5	13.5
Cycle 3	80.9	12.7	93.6	86.4	13.6
Cycle 1	102.9	4.9	107.7	95.5	4.5
Reference North	44.8	4.5	49.2	91	9
Reference South	61.0	5.4	66.4	91.8	8.2

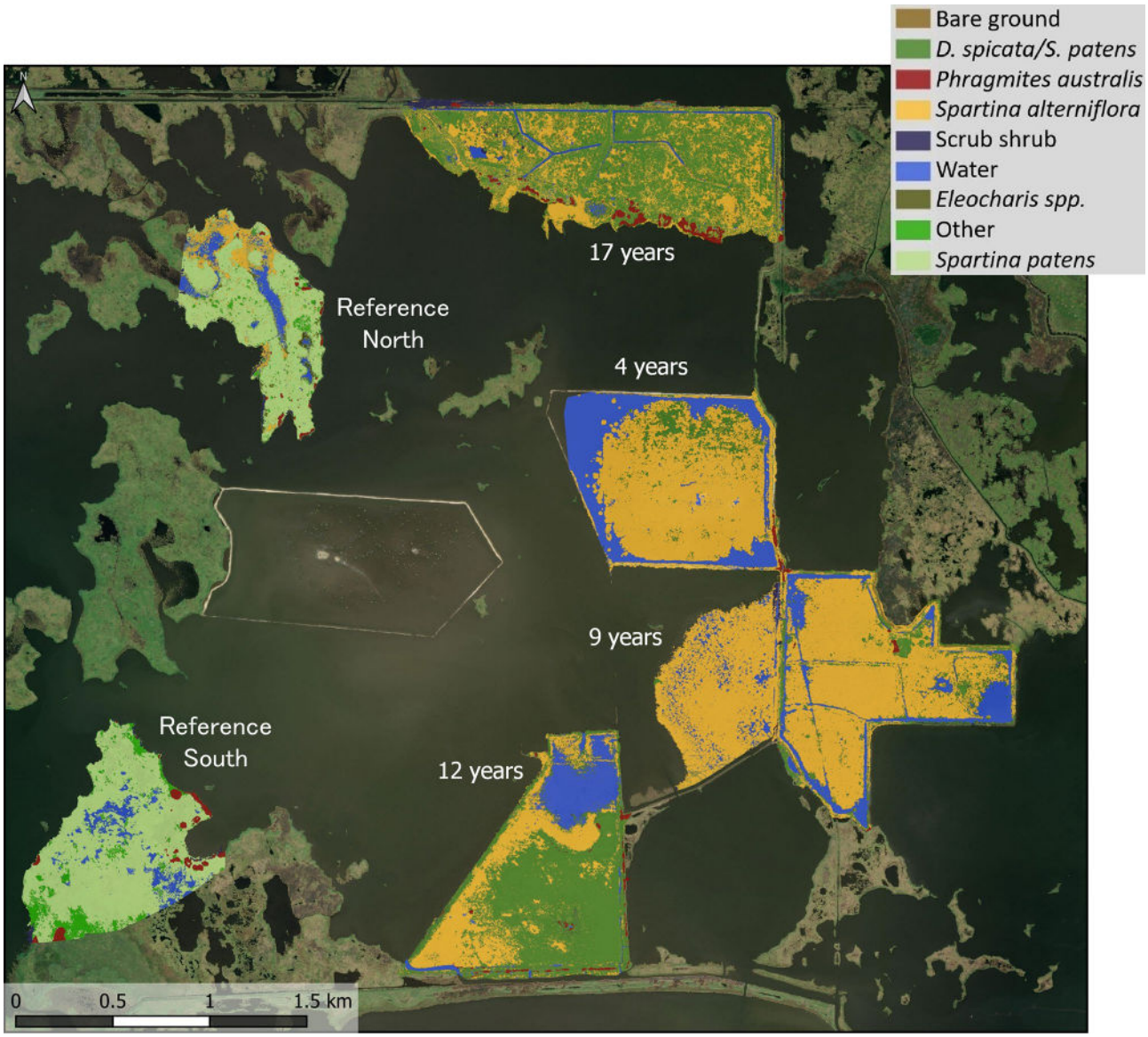

Fig. 5 Drone-based vegetation classification maps (years since construction as of 2019)

Cycle 2 had the highest amount of interior and exterior edge habitat; it was the largest site, but it had the most interior edge by 40 km due to success of the overflow technique. Edge habitat was considered the marsh/water border in this study. Cycle 3 had the highest interior/exterior ratio of 7.9. The youngest sites had the three highest ratios, and the oldest restoration site and references had the lowest ratios of 3–4. Edge is a commonly used metric in landscape ecology and is an important driver of consumer biomass in saltmarshes (Minello et al. 1994). Aggregation index (AI) is the frequency with which patch types appear side by side and quantifies the tendency of a patch to appear in large, grouped distributions (McGarigal 2015; Couvillion et al. 2016). The high AI values for our study sites indicate that land and water are very connected to one another and comprise a landscape characterized by low fragmentation. The reference sites and oldest restoration site (Cycle 1) all have the lowest AI value of 98.8 for the water class meaning water bodies are more scattered across those sites. Cycle 1 had the lowest patch density for land and water classes indicating it was a more spatially connected site with less scattered patches of habitat even though the AI values for water were less than other sites. Although Cycle 3 had the highest interior/exterior edge ratio, Cycle 2 had the highest edge density which is more representative of the amount of small channels present on the landscape.

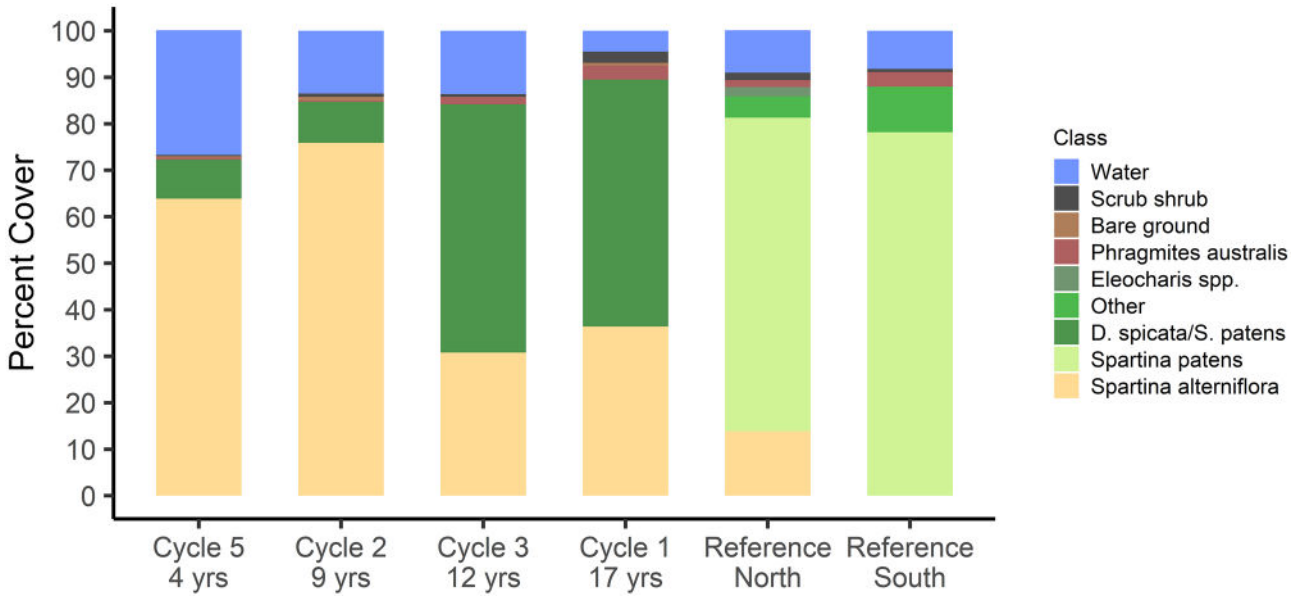

Fig. 6 Drone-based percent cover calculations by species and land cover class

Discussion

The results demonstrate the use of an off-the-shelf drone as a tool to help understand the ecological sequence of restoration and ultimately project success. The high-resolution maps provide a more wholistic perspective of sites than traditional surveys. We quantified how much land was created, how plant community structure shifts with time, and how the hydrology and spatial arrangement of channel networks functions as a result of construction practices thereby informing marsh development. However, determining the highest level of success across projects is not entirely straightforward. Based on manager goals, all four restoration projects were successful in achieving the > 70% land target. Classification results also confirm agency reports that dominant species compositions shift over time from *S. alterniflora* to *D. spicata*/*S. patens*. None of the restored site communities mimic those of reference areas (Fig. 5). And there are potentially tradeoffs to structural configurations and biological characteristics, like less edge habitat but higher species richness with age. It is hard to draw absolute conclusions due to our timeline and construction differences, but sites with more edge habitat and interior water in our study had more *S. alterniflora*. Although a possible function of time in this case, tidal influence does dictate zonation of herbaceous vegetation and *S. alterniflora* is generally more flood tolerant than *S. patens* (Broome et al. 2019; Bertness 1991). In this area, the typical tidal range is approximately 0.5 m semidiurnal tide.

The drone-based estimates for amount-vegetated land aligned with other remote sensing calculations for the oldest restoration site, but there were some significant differences. Most notably, Cycle 3 was the only restored site that showed a decline in the amount of marsh (98% in 2015 to 86% 2019). The northern portion of the cell was shallow open water for the first 5 to 7 years while the rest of the site vegetated (Miller et al. 2019). Personal communication with managers revealed the placement and movement of dredge outflow pipes were improperly executed during construction and left a legacy on site development. The entire site had vegetated by 2015 even though 2018 elevation transects in the northern end were still below target goals (Beck et al. 2019; Miller et al. 2019). Drone imagery from 4 years later showed the same area had returned to open water (Fig. 4). Although 2019 was a year marked by high water levels in south Louisiana, readings at the Cycle 1 hydrology station were similar on the two approximate imagery dates, seriously reducing the chance of flooding bias. It is not certain why the area turned back into water, but these findings highlight the importance of achieving proper elevations in marsh creation projects. Furthermore, vegetation establishment in restored marsh creation sites is not always permanent. Although Suir et al. (2020) demonstrated the resiliency of these sites to past disturbances, restored marsh was lost at Cycle 3, and it will be interesting to see if plants re-establish.

Successes and shortcomings of construction practices were also highlighted by the resolution of drone imagery. Cycle 2 was the only site where the overflow technique was successful thus creating 45 ha of additional marsh but has almost no monitoring data. Personal communication reported it was pumped at too high of an elevation, no details were recorded, and was possibly the reason for the

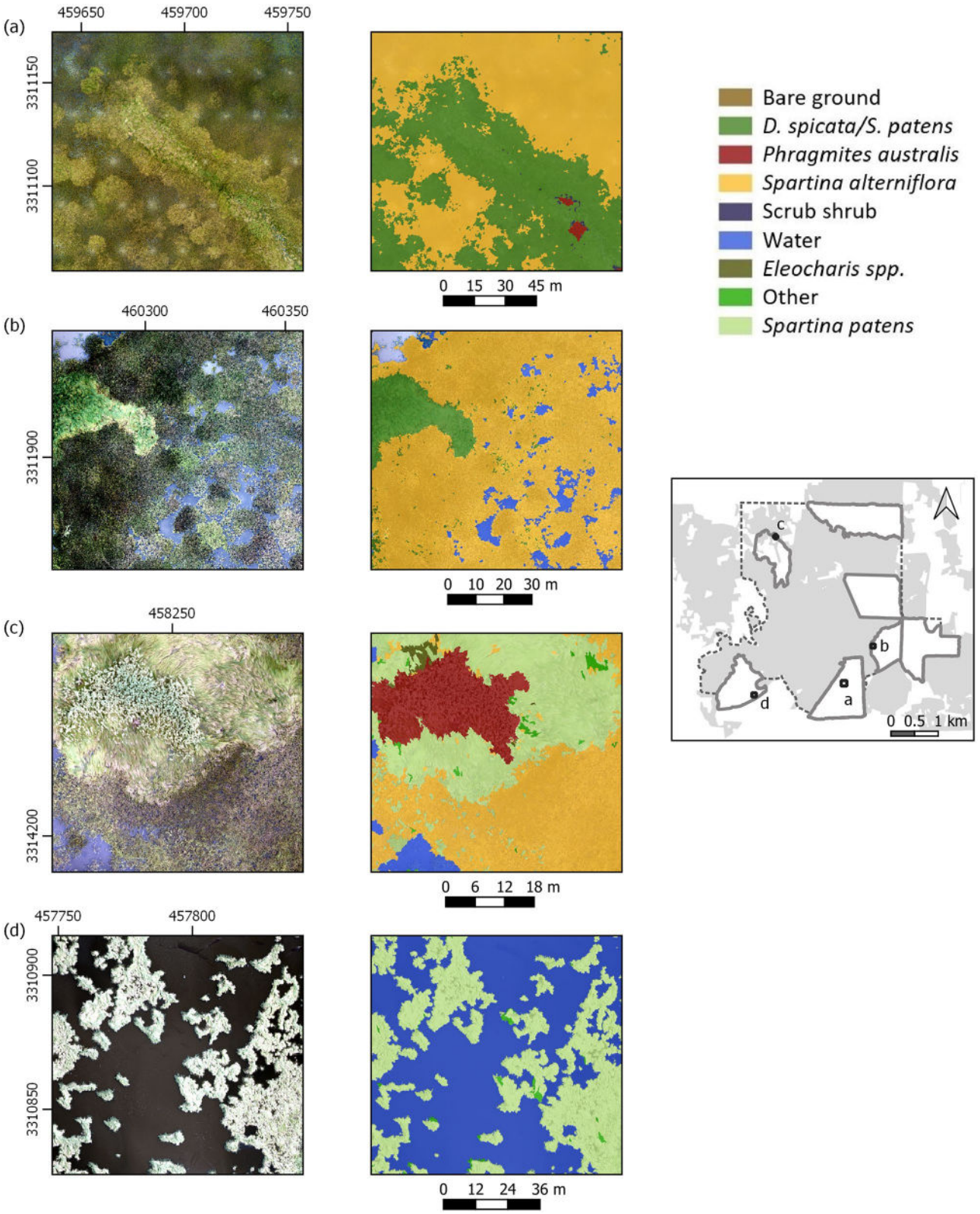

Fig. 7 Images from orthomosaic (left) and corresponding vegetation classification (right) at study sites: Cycle 3 (**a**), Cycle 2 (**b**), Reference North (**c**), and Reference South (**d**)

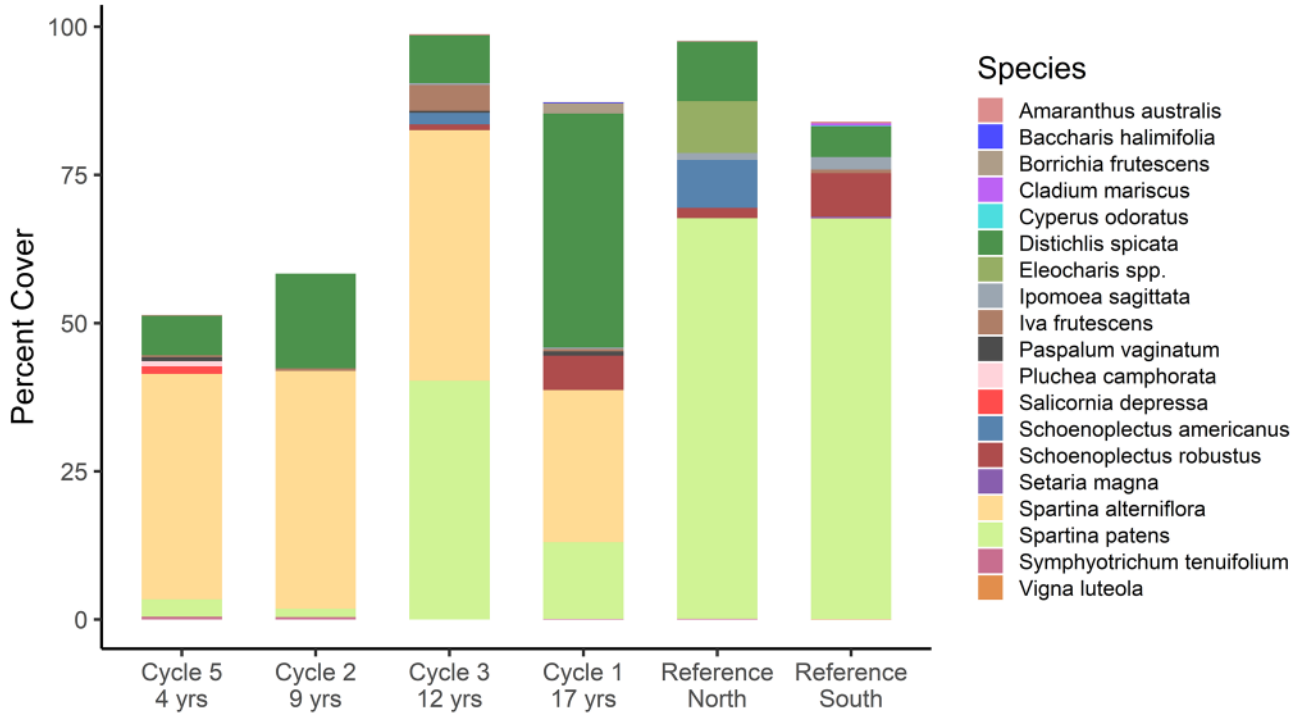

Fig. 8 Field-based percent vegetation cover estimates

overflow success. It was the second youngest site (9 years old) but contained the most land by 30 ha, was within 5% of the reference marsh percent land values, and had the highest amount of interior edge by 40 km. Although plant species diversity was the lowest, the site may be the most beneficial to aquatic organisms. Novel methods used to interpret energy production for white shrimp based on habitat cover demonstrated the importance of edge habitat in these areas as a driver for consumer biomass and abundance (Nelson et al. 2020). Cycle 2 was the most successful project based on manager goals for land creation and perhaps species diversity will develop as the site matures.

Our primary objective was to demonstrate a method using OBIA to classify marsh habitats and develop a workflow that others can build upon to assess future restoration efforts. Further analysis to refine classification techniques would improve classifications and likely lead to more in-depth species maps. We used RGB orthomosaics and elevation information from digital surface models (DSMs) to identify water, bare ground, *Phragmites australis*, and shrubs

Table 2 Land/water calculations from drone imagery (June/July 2019), color infrared aerial photographs (7 December 2015), and WorldView-3 satellite imagery (13 February 2016)

Site	Total area (ha)	Land (ha)	Water (ha)	% land	% water
Cycle 5 Aerial Photo (2015)	93.9	59.9	34.0	63.8	36.2
Cycle 5 Satellite (2016)	94.2	27.1	67.08	28.8	71.2
Cycle 5 UAS (2019)	91.3	66.6	24.7	73	27
Cycle 2 Aerial Photo (2015)	91.1	70.4	20.6	77.3	22.7
Cycle 2 Satellite (2016)	92.6	74.5	18.1	80.4	19.6
Cycle 2 UAS (2019)	90.1	76.1	14.0	84.5	15.5
Cycle 3 Aerial Photo (2015)	90.2	88.2	2.0	97.8	2.2
Cycle 3 Satellite (2016)	95.2	89.6	5.6	94.1	5.9
Cycle 3 UAS (2019)	90.5	77.9	12.6	86.1	13.9
Cycle 1 Aerial Photo (2015)	96.7	91.1	5.7	94.1	5.9
Cycle 1 Satellite (2016)	94.4	90.1	4.2	95.5	4.5
Cycle 1 UAS (2019)	93.7	89.2	4.5	95.2	4.8

using threshold values and then applied a supervised nearest neighbor classification for the remaining vegetation using training samples. Methods were based on previous studies of wetlands, and the general framework should apply to similar habitats but certain differences between in our rulesets highlight the subjectivity of site-specific object-based classification approaches (Broussard et al. 2022; Husson et al. 2016; Laliberte and Rango 2009; Dronova 2015; Pande-Chhetri et al. 2017). For example, the spectral difference segmentation algorithm scale had to be reduced at one site because it grouped a large section of two different plant species together. This reduction made the object sizes smaller leading to an increased processing time of 6 to almost 24 h for the nearest neighbor classifier. Smaller objects also led to more misclassifications at some sites.

OBIA is a powerful technique and has many advantages over pixel-based approaches, but ruleset and feature selection can vary widely depending on the user, type of imagery, time of day, and many other factors. The DSM information was also critical in this study, especially for classifying *Phragmites*; however, some portions of the models were flawed, and open water can create extreme high and low elevation values with drone imagery. We worked around these issues by targeting specific sections of each site when using height data to identify *Phragmites*. The issue may have been a product of our aircraft's internal GPS vertical accuracy and perhaps the addition of more ground control points, especially around stands of *Phragmites*, or the use of Post-Processing Kinematics GNSS hardware on high-precision UAS platforms would have improved our models.

We demonstrated the use of an off-the-shelf multi-rotor aircraft for relatively large 90 + ha (220 acre) site surveys from a boat; although fixed-wing aircrafts are more suited for larger areas, wetlands may not have favorable landing ground. There is also a lower barrier to entry with multi-rotor aircrafts for those interested in integrating drones into their research, and the goal here was to demonstrate the accessibility of drones as a research tool. The ease of piloting, ability to hover, and improvements in flight planning software and automation make multi-rotors available to anyone willing to put in the training for coastal surveys. Advanced sensors, for example multispectral cameras that can capture near-infrared and red edge bands, have been widely used for vegetation studies and benefit analysis of wetland plant health through indices like the normalized difference vegetation index (Broussard et al. 2018), but these are not always available to researchers. Most multi-rotor drones come equipped with an integrated high-resolution RGB camera that, paired with modern processing techniques, can generate powerful datasets for studying logistically difficult areas.

By combining remote sensing and field surveys, we were able to better understand restoration success through accurate water and vegetation mapping, land creation analysis, and spatial arrangement metrics. All sites reached manager goals of 70% land composition, but the sediment overflow technique made one site the most successful. Restored wetlands displayed a general trend of increasing species diversity with age and a shift in dominant species after about 10 years. *Spartina alterniflora* dominated younger sites and was more common in flooded areas with more edge habitat at all sites. Although vegetation communities do not mimic those of reference marshes, spatial metrics and fragmentation indices indicate that restoration sites become equally or more aggregated than natural marshes after about 15 years. Drone imagery also revealed subtle differences in site development that were not captured by previous monitoring data. For example, the expansion of *D. spicata*/*S. patens* was observed in the drone imagery in the northern portion of Cycle 5 after just 4 years.

High-resolution drone imagery helps us understand ecosystem function because of the high fidelity of the imagery and the precision of the spatial positioning, providing a wholistic dataset at the project or site level. Field surveys are essential to determine species composition, but that same data can be used to create realistic habitat configurations by pairing it with drone surveys and training software instead of extrapolating from plot transects. The detail of the imagery gives any user the ability to delineate dominant marsh species across sites and investigate how plant configurations were structured in relation to fine-scale water bodies and channels. We also accurately mapped the invasive species *Phragmites australis* which was underrepresented in previous field surveys. *Phragmites* helps some marshes persist, and dense stands can trap sediment and build land, but major die-offs have occurred in coastal LA because of an invasive scale insect from Asia and other reasons leading to a significant increase in research on the subject. Samiappan et al. (2016) also demonstrated the utility of drones for mapping *Phragmites*. In general, processing methods were time consuming, but continual refinement will speed up the process, and techniques could eventually be adopted and standardized for this region. The imagery can also serve as a baseline for future research because although previous remote sensing studies have been conducted at the sites, the resolution of the drone imagery is significantly higher than any other source.

Future studies using drones to survey marshes should consider a few changes to our approach. Project objectives and questions generally determine methodological parameters, and there are tradeoffs to different approaches. For example, one could fly at a slightly higher altitude to reduce the number of images and speed up processing time, but you would lose resolution. We chose to fly at 68-m altitude to achieve 2.2-cm pixel resolution on the ground. A GSD of 2.5 cm or slightly higher would be sufficient for this analysis, resulting in a higher altitude flight plan, fewer images to analyze, and

less time post-processing. Another consideration is sun glare on open water. We would suggest flying earlier in the morning to reduce sun glare and make the classification of water easier. This approach is acceptable in the largely herbaceous marshes where long shadows are not present due to the lack of taller objects in the landscape. Lower wind and sun glare make the use of textural and spectral features more effective when using RGB imagery. OBIA segmentation scale parameters and the combination of multiresolution and spectral difference algorithms worked very well for delineating water across sites, but scales were not as consistent for delineating marsh grasses. The maximum spectral difference scale of 10 worked for some sites, but it had to be reduced for others so that different species were not grouped together. Unfortunately, this reduction led to a higher number of smaller objects and more misclassifications.

Drones have revolutionized spatial ecology, and the technology's use has rapidly increased across many scientific disciplines because of its operational flexibility, high-quality/low-cost data, and repeatability (Anderson and Gaston 2013). The current regulatory environment managed by the FAA and user-friendly flight planning software makes using drones a viable option for any researcher. No other remote sensing method offers such high detail for the price. The biggest caveat is processing time, but methodological refinement and advancements in computing and software packages will continually reduce the temporal burden. Coastal research would significantly benefit from increased use of the technology and efforts to improve automated processing techniques.

References

Anderson, K., and K. J. Gaston. 2013. Lightweight unmanned aerial vehicles will revolutionize spatial ecology. *Frontiers in Ecology and the Environment* 11: 138–146.

Baatz, M., and A. Schäpe. 2000. Multiresolution segmentation: an optimization approach for high quality multi-scale image segmentation. *Angewandte Geographische Informationsverarbeitung* XII: 12–23.

Barbier, E.B., S.D. Hacker, C. Kennedy, E.W. Koch, A.C. Stier, and B.R. Silliman. 2011. The value of estuarine and coastal ecosystem services. *Ecological monographs* 81 (2): 169–193.

Beck, H., K. Mouton, J. Dugas, and B. Couvillion. 2019. *Sabine Refuge Marsh Creation (CS-28): 2015 land-water classification*. Raster Digital Data Set U.S.: Geological Survey. https://doi.org/10.5066/P95K89ZU.

Bertness, M.D. 1991. Zonation of Spartina patens and Spartina alterniflora in New England salt marsh. *Ecology* 72: 138–148.

Boesch, D.F., M.N. Josselyn, A.J. Metha, J.T. Morris, W.K. Nuttle, C.A. Simenstad, and D.J. Swift. 1994. Scientific assessment of coastal wetland loss, restoration and management in Louisiana. *Journal of Coastal Research*, 103.

Boon, M.A., R. Greenfield, and S. Tesfamichael. 2016. Unmanned aerial vehicle (UAV) photogrammetry produces accurate high-resolution orthophotos, point clouds and surface models for mapping wetlands. *South African Journal of Geomatics* 5 (2): 186–200.

Broome, S.W., C.B. Craft, and N.R. Burchell. 2019. idal marsh creation. In *In: Coastal wetlands: an integrated ecosystem approach.*, ed. G.M.E. Perillo, E. Wolanski, D.R. Cahoon, and C.S. Hopkinson, 789–876. Elsevier.

Broussard, III WP, G. Suir, and J. Visser. 2018. Unmanned Aircraft Systems (UAS) and satellite imagery collections in a coastal intermediate marsh to determine the land-water interface, vegetation types, and normalized difference vegetation index (NDVI) values. Engineer research and development center: wetlands regulatory assistance program technical note 18(1):1–17. Vicksburg, MS: U.S. Army Engineer Research and Development Center. https://doi.org/10.21079/11681/29517.

Broussard, W.P., III., J.M. Visser, and R.P. Brooks. 2022. Quantifying vegetation and landscape metrics with hyperspatial unmanned aircraft system imagery in a coastal oligohaline marsh. *Estuaries and Coasts* 45: 1058–1069. https://doi.org/10.1007/s12237-020-00828-8. shallow water mapping special issue.

Coastal Protection and Restoration Authority of Louisiana. 2023. Louisiana's comprehensive master plan for a sustainable coast. Coastal protection and restoration authority of Louisiana. Baton Rouge, LA.

Colomina, I., and P. Molina. 2014. Unmanned aerial systems for photogrammetry and remote sensing: A review. *ISPRS Journal of photogrammetry and remote sensing* 92: 79–97.

Congalton, R. G. 1991. A review of assessing the accuracy of classifications of remotely sensed data. *Remote Sensing of Environment* 37: 35–46.

Couvillion, B.R., Barras, J.A., Steyer, G.D., Sleavin, W., Fischer, M., Beck, H., Trahan, N., Griffin, B. and Heckman, D., 2011. Land area change in coastal Louisiana from 1932 to 2010.

Couvillion, B. R. et al. 2016. Spatial configuration trends in coastal Louisiana from 1985 to 2010. *Wetlands* 36: 347–359.

Couvillion, B.R., Beck, H., Schoolmaster, D. and Fischer, M., 2017. Land area change in coastal Louisiana (1932 to 2016) (No. 3381). US Geological Survey.

Costanza, R., O. Pérez-Maqueo, M.L. Martinez, P. Sutton, S.J. Anderson, and K. Mulder. 2008. *The value of coastal wetlands for hurricane protection*, 241–248. Ambio.

Cowardin, L.M., 1979. Classification of wetlands and deepwater habitats of the United States. Fish and Wildlife Service, US Department of the Interior.

Cretini, K. F. et al. 2011. Development and use of a floristic quality index for coastal Louisiana marshes. *Environmental Monitoring and Assessment* 184: 2389–2403.

Cretini, K.F., J.M. Visser, K.W. Krauss, and G.D. Steyer. 2012. Development and use of a floristic quality index for coastal Louisiana marshes. *Environmental monitoring and assessment* 184: 2389–2403.

Crossett, K., Ache, B., Pacheo, P., Haber, K. 2013 National Coastal Population Report: Population Trends from 1970 to 2020. NOAA State of the Coast Report Series 19 pp.

Doughty, C.L., and K.C. Cavanaugh. 2019. Mapping coastal wetland biomass from high resolution unmanned aerial vehicle (UAV) imagery. *Remote Sensing* 11 (5): 540.

Dronova, I. 2015. Object-based image analysis in wetland research: a review. *Remote Sensing* 7: 6380–6413.

Enwright, N.M., W.R. Jones, A.L. Garber, and M.J. Keller. 2014. Analysis of the impact of spatial resolution on land/water classifications using high-resolution aerial imagery. *International Journal of Remote Sensing* 35 (13): 5280–5288.

Folse, T.M., West, J.L., Hymel, M.K., Troutman, J.P., Sharp, L.A., Weifenbach, D., McGinnis, T., Rodrigue, L.B., Boshart, W.M., Richardi, D.C. and Miller, C.M., 2014. A standard operating procedures manual for the Coast-wide Reference Monitoring System. Wetlands: Methods for Site Establishment, Data Collection, and Quality Assurance/quality Control. Coastal Protection and Restoration Authority, Baton Rouge, LA, p.228.

Forsmoo, J. et al. 2019. Structure from motion photogrammetry in ecology: does the choice of software matter? *Ecology and Evolution* 9: 12964–12979.

Gianopulos, K., 2014. Coefficient of Conservatism database development for wetland plants occurring in the Southeastern United States. North Carolina Dept. of Environment & Natural Resources, division of water resources: wetlands branch. Report to the EPA, region, 4.

Hunt, E. R. et al. 2005. Evaluation of digital photography from model aircraft for remote sensing of crop biomass and nitrogen status. *Precision Agriculture* 6: 359–378.

Husson, E., F. Ecke, and H. Reese. 2016. Comparison of manual mapping and automated object-based image analysis of non-submerged aquatic vegetation from very-high-resolution UAS images. *Remote Sensing* 8: 1–18.

Husson, E., H. Reese, and F. Ecke. 2017. Combining spectral data and a DSM from UAS-images for improved classification of non-submerged aquatic vegetation. *Remote Sensing* 9 (3): 247.

Kalacska, M., G.L. Chmura, O. Lucanus, D. Bérubé, and J.P. Arroyo-Mora. 2017. Structure from motion will revolutionize analyses of tidal wetland landscapes. *Remote Sensing of Environment* 199: 14–24.

Klemas, V. 2015. Remote sensing of floods and flood-prone areas: An overview. *Journal of Coastal Research* 31 (4): 1005–1013.

Laliberte, A.S., and A. Rango. 2009. Texture and scale in object-based analysis of subdecimeter resolution unmanned aerial vehicle (UAV) imagery. *IEEE Transactions on Geoscience and Remote Sensing* 47 (3): 761–770.

Laliberte, A. S., and A. Rango. 2011. Image processing and classification procedures for analysis of sub-decimeter imagery acquired with unmanned aircraft over arid rangelands. *GIScience & Remote Sensing* 28: 4–23.

Lopez, R. D., and M. S. Fennessy. 2002. Testing the floristic quality assessment index as an indicator of wetland condition. *Ecological Applications* 12: 487–497.

Coastal Protection and Restoration Authority of Louisiana. 2012. Louisiana's Comprehensive Master Plan for a Sustainable Coast. Coastal Protection and Restoration Authority of Louisiana. Baton Rouge, LA.

Manfreda, S. et al. 2019. Assessing the accuracy of digital surface models derived from optical imagery acquired with unmanned aerial systems. *Drones* 3: 15.

McGarigal, K., 2015. FRAGSTATS help. University of Massachusetts: Amherst, MA, USA, 182.

Millennium Ecosystem Assestment. 2005. *Ecosystem and human well-being: wetland and water synthesis*. Washington DC: World Resources Institute.

Miller, M., 2014. Operations, Maintenance, and Monitoring Report for Sabine Refuge Marsh Creation (CS-28). Coastal protection and restoration authority of Louisiana, coastal protection and restoration, Lafayette, Louisiana. 25pp.

Miller, M., Guidry, M., White, J. . 2019 Short summary report: sabine refuge marsh creation Cycles - 3-4-5. Coastal protection and restoration authority of Louisiana, Coastal protection and restoration, Baton Rouge, Louisiana. 2pp. Vancouver

Minello, T. J., R. J. Zimmerman, and R. Medina. 1994. The importance of edge for natant macrofauna in a created salt marsh. *Wetlands* 14: 184–198.

Mitsch, W.J., and J.G. Gosselink. 2015. *Wetlands*. John Wiley & sons.

Mitsch, W.J., B. Bernal, A.M. Nahlik, Ü. Mander, L. Zhang, C.J. Anderson, and H. Brix. 2013. Wetlands, carbon, and climate change. *Landscape ecology* 28: 583–597.

Nelson, J.A., et al. 2020. (In review) new mapping metrics to test functional response of food webs to coastal restoration. *Food Webs in Review* 25: e00179.

Oniga, V.E., A.I. Breaban, and F. Statescu. 2018. Determining the optimum number of ground control points for obtaining high precision results based on UAS images. *Proceedings* 2 (7): 352.

Pande-Chhetri, R. et al. 2017. Object-based classification of wetland vegetation using very high-resolution unmanned air system imagery. *European Journal of Remote Sensing* 50: 564–576.

Pontiff, D.J., White, J.R. 2017. 2016/2017 Annual Inspection Report Sabine Refuge Marsh Creation Project (CS-28-4&5). Coastal Restoration and Protection Authority. Lafayette, LA

Samiappan, S. et al. 2016. Using unmanned aerial vehicles for high-resolution remote sensing to map invasive Phragmites australis in coastal wetlands. *International Journal of Remote Sensing* 38: 2199–2217.

Sharp, L.A. 2011 operations, maintenance, and monitoring report for Sabine Refuge Marsh Creation. Coastal Protection and Restoration Authority of Louisiana, Coastal Protection and Restoration, Lafayette, Louisiana. 25pp.

Suir, G.M., and C.E. Sasser. 2017. *Floristic quality index of restored wetlands in Coastal Louisiana. Ecosystems Management Restoration Research Program*. Washington D.C.: U.S. Army Corps of Engineers Engineer Research and Development Center.

Suir, G.M., Sasser, C.E. and Harris, J.M., 2020. Use of remote sensing and field data to quantify the performance and resilience of restored Louisiana wetlands. Wetlands, 40(6), pp.2643-2658.

Weinstein, M.P., J.M. Teal, J.H. Balletto, and K.A. Strait. 2001. Restoration principles emerging from one of the world's largest tidal marsh restoration projects. *Wetlands Ecology and Management* 9: 387–407.

Zweig, C.L., M.A. Burgess, H.F. Percival, and W.M. Kitchens. 2015. Use of unmanned aircraft systems to delineate fine-scale wetland vegetation communities. *Wetlands* 35: 303–309.